UNIVERSITÀ DEGLI STUDI DI PADOVA
DIPARTIMENTO DI INGEGNERIA CIVILE, EDILE E AMBIENTALE
Department of Civil, Environmental and Architectural Engineering

Corso di Laurea in Ingegneria per l'Ambiente e il Territorio

Tesi di laurea

THE IMPACT OF CLIMATE CHANGE ON SALENTO'S URBAN TERRITORIES: MAPPING AND ANALYSIS ON URBAN HEAT ISLANDS INTENSITY

Relatore: prof. Salvatore Pappalardo
Co-tutor: dott. Carlo Zanetti

Laureando: Stefano De Razza

ANNO ACCADEMICO 2022-2023

Abstract

Land surface temperature (LST) is a fundamental variable for climate change studies and for monitoring temperature anomalies. At the urban scale, this variable is widely used to study the phenomenon of urban heat islands (UHI). The analysis of the LST proposed in this study focuses on the Salento area in Southern Italy during a heatwave and shows a completely anomalous behaviour, which is not consistent with the phenomenon of microclimatic urban heat islands. The analysed urban areas seem to be characterised by a lower temperature than the surrounding poorly vegetated fields and rural areas. The purpose of the study is to understand which factors contribute to this anomaly and to demonstrate the possible existence of a relation between temperature, land use, vegetation and surface albedo through statistical analysis of Landsat-8 satellite images processed by a GIS software.

Keywords: urban heat islands, climate change, LST, Landsat-8, QGIS

Index

1. Introduction

1.1 Heat waves

Due to the increased greenhouse gas concentrations in the atmosphere, human-induced global warming is worsening the magnitude and frequency of heatwaves (Wehrli et al., 2019). Heat waves cause consequences on socio-environmental systems, including hydrological and agricultural resources and energy supplies (Beniston et al., 2007). They are responsible for serious heat-related health issues and they can lead to a large number of deaths (Oudin Åström et al., 2015). Many studies investigating impacts of heat waves in Europe have found a critical increase in total daily mortality for all natural deaths, especially for mortality from respiratory, cardiovascular and cerebrovascular diseases, with higher impacts in Mediterranean cities (D'ippoliti et al., 2010). Climate extremes such as heatwaves have globally increased in recent decades; climate models show that the Mediterranean region is a global warming hotspot (Diffenbaugh et al., 2007), by increasing the average temperature at a rate about 20% higher than the global annual mean surface temperature (Lionello & Scarascia, 2018). This trend is expected to intensify, by increasing average and extreme temperatures as well as the frequency and duration of heat waves (Spano, 2020). Southern European cities will face an increase in heatwaves events and drought severity, with future droughts up to 14 times worse than those in the past (Guerreiro et al., 2018). Drought also affects vegetative state by reducing the photosynthetic activity of plants (Yang et al., 2021), leading to a decline in crop productivity. Some vegetation species can also be killed by temperatures approaching 40°C. In addition, forest ecologists have recognised that extreme drought conditions weaken and stress trees, making them more susceptible to insect attacks and diseases (Schlesinger et al., 2016); and in particular in southern Europe, for both tree and herbaceous crops. As a result, many fields are expected to become unused or openly exposed to direct solar radiation, therefore absorbing more solar radiation than vegetated areas (Ghosh & Das, 2018) and having a higher surface temperature (Ni et al., 2019).

1.2 Urban Heat Island

In most cases, urban environments are characterised by a complex urban fabrique combining impervious surfaces such as concrete and asphalt with permeable and vegetated surfaces. Such impermeable surfaces are generally more prone to absorbing solar radiation and maintaining heat (Spano, 2020), making densely populated cities 5 to 10 °C warmer than surrounding rural areas.

This is known as the urban heat island (UHI) effect and it is one of the most representative phenomena of urban climate (Kim & Brown, 2021). This temperature increase is directly correlated to the size of the city centre, the main building types (Naumann & Formetta, 2020), the salient features intended as urban materials, the greenery, the urban morphology such as the presence of urban canyons, the population density (Sangiorgio et al., 2020), the geography of the city location and topographical features, presence of water bodies, properties of soils (Oke, 1982), climatic conditions and seasonal variations (Mohajerani et al., 2017). All possible combinations of these parameters can create different conditions that may be beneficial or detrimental to city dwellers. In most cases, densely populated urban areas are significantly warmer than surrounding non-urbanised areas. In contrast, a study of some cities in the United States showed that cities built in arid or desert-like environments may experience lower temperatures than surrounding areas, as the urban cores are greener than their surroundings (Bounoua et al., 2015). The thermal difference between urban and rural areas is mainly studied through satellite remote sensing. Many authors have documented the use of satellite remote sensing for the purpose of assessing surface temperature (LST) and UHI spatial and temporal variability mitigation (Liu & Zhang, 2005), while other scholars have evaluated the relationship between different vegetation indices and LST (Kumar & Shekhar, 2015) or between different land uses and LST (Kumar & Shekhar, 2015).

1.3 Urban Heat Island Mitigation

As approximately three quarters of the European population live in cities, mitigation measures are essential to minimize the impact of UHI (Naumann & Formetta, 2020). Mitigation measures have been studied and implemented over the years, with many studies focusing on the albedo, permeability, density, and water retention of urban pavements, as these properties have a significant impact on surface temperature (Mohajerani et al., 2017). In particular, albedo represents the ability to reflect solar radiation (Sangiorgio et al., 2020), it varies between 0 and 1 (the more reflective a surface is the higher the albedo value) and it has been shown that increasing the albedo of urban settlements can reduce temperatures (Akbari et al., 2012). This cooling is especially important in cities with hot climates. Albedo values for urbanised areas typically range from 0.10 to 0.20. Some exceptions can be found in some towns in North Africa, where albedo values can range from 0.30 to 0.45 (Taha, 1997). In addition, green spaces such as grasslands, short vegetation, and trees have another significant effect because they can control soil temperature through evapotranspiration (Armson et al., 2012; Souch & Souch, 1993). In fact, evaporative cooling could play an important role in future sustainable urban expansion.

2. *Data and Methods*

In this study, climate analyses to detect heatwaves were performed by using Microsoft Excel ©, satellite data were modelled and geovisualized in an open source GIS ecosystem (QGIS, v. 3.28.2), and satellite imagery was processed using R software and RStudio interface.

2.1 Study Area

The study is framed on two scales of analyses: on the city and Province of Lecce. It is located in the middle of the Salento peninsula, in south-eastern Italy (Fig. 1). With an area of over 2.798,8 km^2 (Istituto Nazionale di Statistica, 2020), the Province of Lecce is one of the most populous and densely populated provinces in Southern Italy, with a settlement system characterised by the presence of numerous small towns. The subsoil of Salento is devoid of any resources except for the huge deposits of sedimentary rock known as "pietra leccese". In fact, rocks are mainly composed of carbonates, and karst phenomena hinder the development of surface hydrological networks.

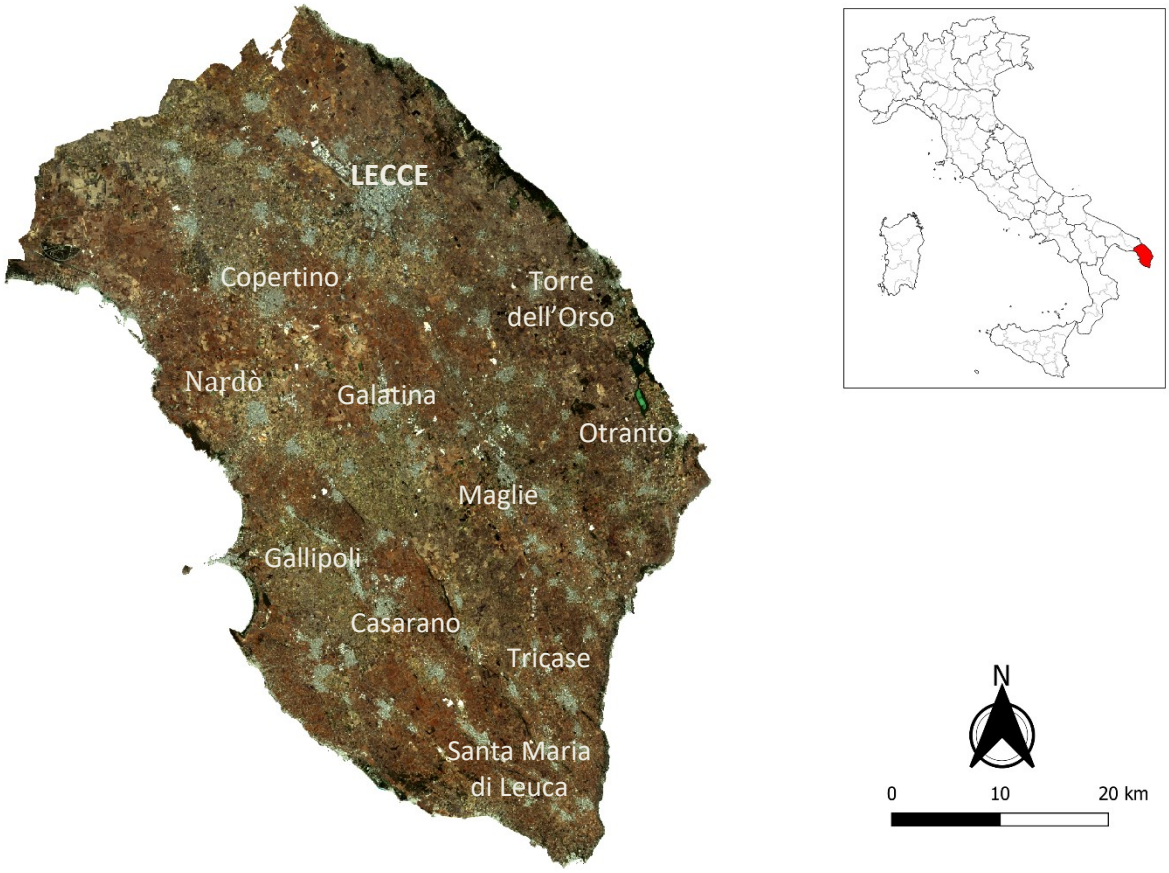

***Figure 1**: Study Area, the Province of Lecce.*

2.2 Weather Data

The meteorological data used in the first part of this work were recorded by the Lecce Galatina weather station and collected by the National Center for Environmental Information (NCEI), one of the most important atmospheric data archives. The study used all daily maximum temperatures from 1992 to 2022.

2.3 Landsat-8 Data

Landsat-8 was launched on February 11th, 2013 with two Earth imaging sensors on-board: the Operational Land Imager (OLI) and the Thermal Infrared Sensor (TIRS). The OLI measures in the visible, near infrared, and shortwave infrared portions (VNIR, NIR, and SWIR) of the spectrum. The TIRS measures land surface temperature in two thermal bands (*USGS*, n.d.). Band designations of Landsat-8 are listed in Table 1.

***Table 1**: Landsat-8 OLI and TIRS.*

Band	Wavelength (micrometres)	Resolution (metres)
1 - Coastal Aerosol	0.43 - 0.45	30
2 - Blue	0.45 - 0.51	30
3 - Green	0.53 - 0.59	30
4 - Red	0.64 - 0.67	30
5 - NIR	0.85 - 0.88	30
6 - SWIR 1	1.57 - 1.65	30
7 - SWIR 2	2.11 - 2.29	30
8 - PAN	0.50 - 0.68	15
9 - Cirrus	1.36 - 1.38	30
10 - TIRS 1	10.6 - 11.19	100
11 - TIRS 2	11.5 - 12.51	100

Multispectral remote sensing imagery of the Salento Peninsula was provided by the United States Geological Survey (USGS) and downloaded from the official geoplatform EarthExplorer.

2.4 Land Cover Data

The Corine Land Cover (CLC) is derived from orthophotos acquired in 2011 with a minimum mapping unit of 0.25 ha, downloaded from the Apulia Region website. The CLC database includes different land use and land cover classes: the man-made surfaces, agricultural surfaces, wooded surfaces and other natural environments of the Apulia Region in the form of vector data and it is used to define vegetated surfaces. Additionally, the 2021 National Land Use Map provided by the "Istituto Superiore per la Protezione e la Ricerca Ambientale" (ISPRA) is used to identify and differentiate between permeable and impermeable surfaces.

2.5 Urban Heat Island Analysis

Although there is no universally accepted definition of a heatwave, there are some statistical criteria and thresholds that have been widely used and tested in the literature. In this study, heatwave days were defined by the Heat Wave Magnitude Index, as the maximum magnitude of the heatwaves in a year, where a heatwave is the period with three or more consecutive days with maximum temperature above the daily threshold for the reference period. The reference period of the study is 31 years baseline, from 1992 to 2022. The threshold is defined as the 90th percentile of the daily maximum temperature, centred on a 31-day window (Russo et al., 2014).

$$A_d = \bigcup_{y=1992}^{2022} \bigcup_{i=day-15}^{day+15} T_{y,i} \quad (1)$$

Where:

- A_d is the threshold;
- ∪ is the union of datasets;
- T_y is the daily T_{max} of the year y and the day i.

2.6 Data Processing

The first step in the work was to convert Digital Number (DN) values to Top Of Atmosphere (TOA) Reflectance (for bands 2, 3, 4, 5, 6, 7) by using the semi-automatic classification plugin on QGIS, and to TOA Radiance (for band 10) using the RS&GIS plugin. After converting DN values to TOA Radiance, the TIRS band data were converted to brightness temperature (BT) using the thermal constants and the formula published in USGS Landsat 8 product:

$$BT = \frac{K_2}{ln\left[\left(\frac{K_1}{L_\lambda}\right) + 1\right]} - 273.15 \quad (2)$$

Where:

- K_2 and K_1 are the thermal constants of TIR band 10 extracted by the metadata file;
- L_λ is the at-sensor spectral radiance.

The obtained result is expressed in degrees centigrade.

One of the methods for calculating emissivity is based on the Normalized Difference Vegetation Index (NDVI), which is crucial for mapping and classifying land cover types in the study area. NDVI values vary from -1 to 1. In general, NDVI values range from -1 to 0 for water bodies, -0.1 to 0.1 for bare or sandy land, 0.2 to 0.5 for mixed vegetation or degraded soil, shrubs or grass crops and from 0.6 to 1.0 for dense vegetation (Kshetri, 2018). NDVI is calculated as the normalized difference between TOA spectral reflectance in OLI infrared (R_{NIR}) and red (R_{RED}) using the following formula:

$$NDVI = \frac{(R_{NIR} - R_{RED})}{(R_{NIR} + R_{RED})} \quad (3)$$

With the obtained NDVI values, it is possible to calculate the proportional vegetation (P_v) as follows (Narayana Reddy & Manikiam, 2017):

$$P_v = \left(\frac{NDVI - NDVI_s}{NDVI_v - NDVI_s}\right)^2 \quad (4)$$

Where:

- $NDVI_s$ is the NDVI for the barren soil pixel;
- $NDVI_v$ is the NDVI for the fully vegetated pixel.

The Land surface emissivity (LSE) is the average emissivity of an element on the surface of the Earth estimated using NDVI threshold method (Rajeshwari & Mani N, 2014).

$$LSE = \varepsilon_s(1 - P_v) + \varepsilon_v * P_v \quad (5)$$

Where:

- ε_s is the soil emissivity value of band 10;
- ε_v is the vegetative emissivity value of band 10;
- $P_v\ is\ the$ proportional vegetation.

The Land Surface Temperature (LST) is the radioactive temperature and it is calculated as follows (Stathopoulou & Cartalis, 2007):

$$LST = \frac{BT}{\{1 + [(\frac{\lambda BT}{\rho})\ ln(LSE)]\}} \quad (6)$$

Where:

- BT is at-sensor brightness temperature (°C);
- λ is the wavelength of emitted radiance (λ = 10.895 μm);
- LSE is the emissivity;
- ρ = (h * $\frac{c}{\sigma}$) = 1.438 × 10^{-2} m K, where σ is the Boltzmann constant, h is the Plank's constant and c is the speed of light.

LST is expressed in degree centigrade.

The surface albedo (SA) can be estimated using Eq. (7) (Cunha et al., 2020):

$$SA = b_{BLUE} * \rho_{BLUE} + b_{GREEN} * \rho_{GREEN} + b_{RED} * \rho_{RED} + b_{NIR} * \rho_{NIR} + b_{SWIR1} * \rho_{SWIR1} + b_{SWIR2} * \rho_{SWIR2} + b_0 \quad (7)$$

Where:

- ρ are the surface bidirectional reflectance values;
- b are the corresponding conversion coefficients (Tab. 2).

***Table 2**: Band conversion coefficients for Landsat-8.*

b_{BLUE}	b_{GREEN}	b_{RED}	b_{NIR}	b_{SWIR1}	b_{SWIR2}	b_0
0.2453	0.0508	0.1804	0.3081	0.1332	0.0521	0.0011

To perform the surface albedo analysis, a threshold for neglecting the effects of vegetation was applied to the NDVI values, and only pixels with values < 0.3 were selected (Bonafoni et al., 2017). This is done to ignore the opposite effect of evapotranspiration of vegetation on the albedo values.

2.7 Urban Heat Island Intensity Analysis

The thermal anomaly analysis was carried out focusing on Lecce and its adjacent areas. To calculate the thermal anomaly among urban and rural areas we adopted the Oke (1978) methodology combined with a GIS-based approach. From the surface data described in paragraph 2.3, this research focused on the area contained between two circumferences of radius 3 km and 6 km and centred in the geographical centre of Lecce. Within this region, the area was further refined to the only non-urbanised surfaces with their centre point at a minimum of 100 m away from every artificial surface (Todeschi et al., 2022). The areas that satisfy this condition are then sampled at their centre point by calculating the temperature difference (ΔLST) as the difference between the LST value from Eq. (6) and the average temperature value of pixels located in non-urban areas.

3. Results and Discussion

The analysis was carried out at two different scales to describe the phenomenon in the province and in the urban area of Lecce. This section consists of different subsections, each focusing on a specific parameter. It firstly analyses vegetation using the NDVI, followed by LST and urban thermal anomaly. Finally, the Surface Albedo (SA) is analysed.

3.1 Climate Analysis

According to the values recorded by the Lecce Galatina weather station, two heatwaves hit this area in 2022, from June 4th to the 7th and from July 23rd to the 26th, both lasting four days. As a result, a Landsat-8 scene was acquired from USGS database on July 24th, 2022, with a maximum air temperature recorded at the Lecce Galatina weather station of 37.6 °C. This date was not chosen at random, but it was the only day that met certain conditions. Specifically, this day coincided with a heat wave period and presented a clear sky, an essential condition that must be fulfilled to avoid anomalies in the measurement of surface temperature. The scene centre time is 9:29 UTC.

3.2 Normalized Difference Vegetation Index

A mapped version of the obtained vegetation index can better visualize the vegetation distribution in the Salento area (Fig. 2). The values obtained are in a range between -0.58 and 0.80. Poorly densely green covers such as urban areas or bare soil regions are characterised by low NDVI values. They can be identified as brown in the image by a true colour band composition while highly vegetated regions are green. NDVI value is lower in the north-western part of the region, as it is characterised by sparse vegetation in summer months. In many areas it is difficult to distinguish between built-up and vegetated areas as they both have similar values. Vegetation seems to be prevalently present in coastal areas, where the climatic conditions are more appealing to the flourishing growth of flora.

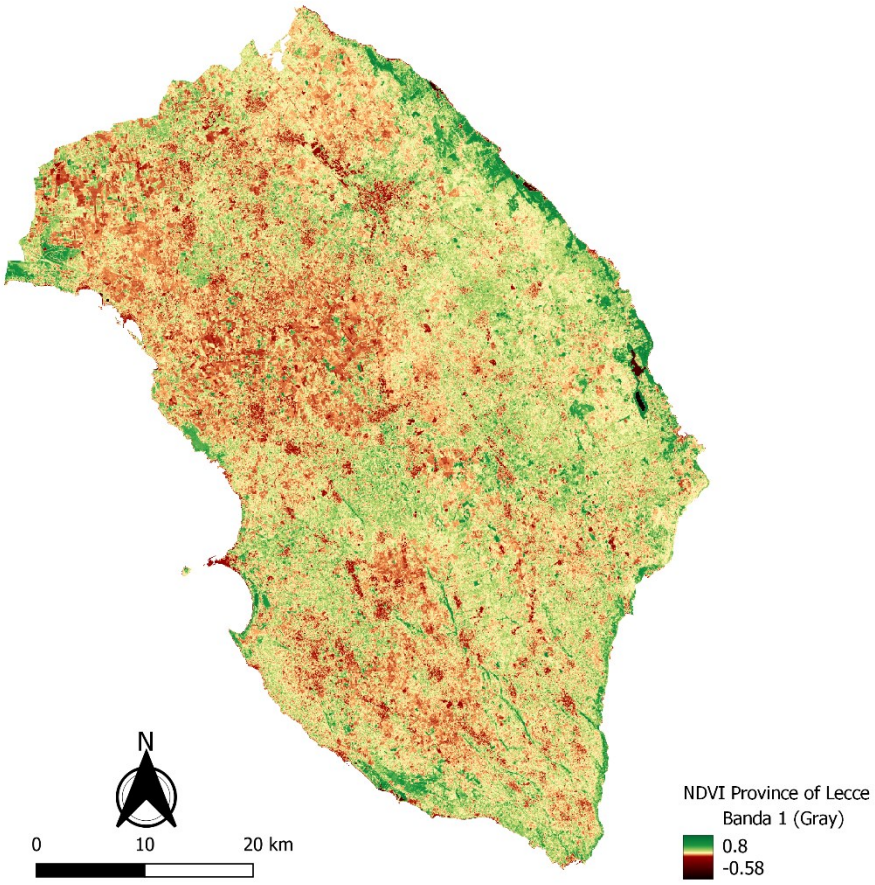

***Figure 2**: NDVI value in the Province of Lecce detected on 24th July, 2022.*

At the city scale, NDVI values were taken from a circular buffer zone with a diameter of 9 km centred at the geographical centre of Lecce (Fig. 3). NDVI values range from -0.11 to 0.74. The lowest values are found in urban areas, especially in the industrial north-west of the city, while the highest values are found in the heavily vegetated area on the north-eastern coastline.

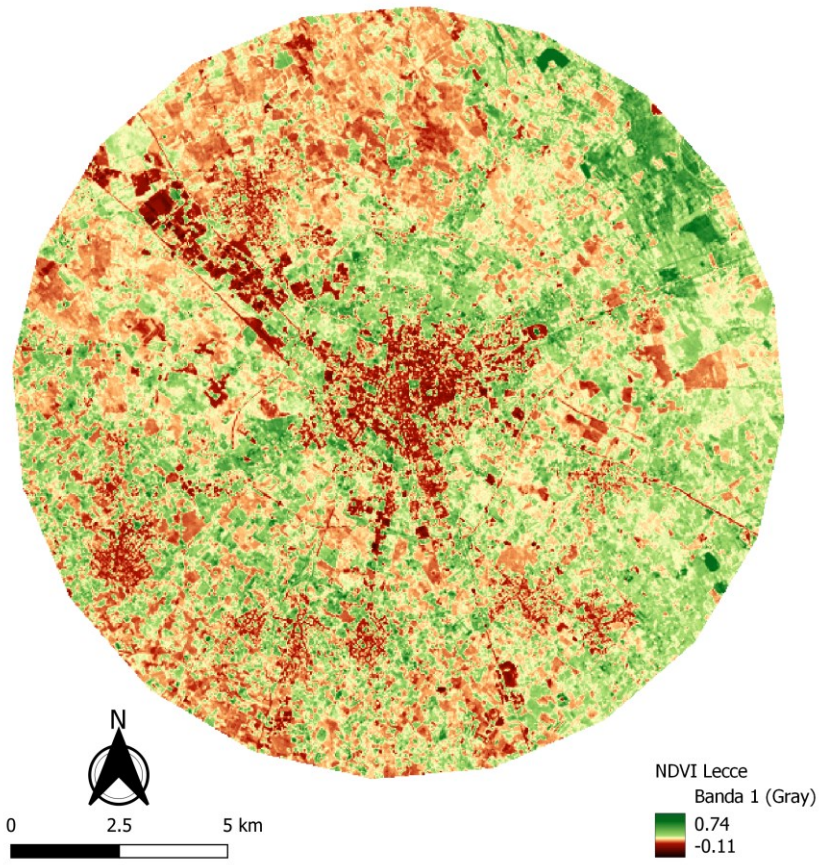

***Figure 3**: NDVI value in Lecce detected on 24th July, 2022.*

3.3 Land Surface Temperature

LST analysis, at the Province scale, showed that urban areas and man-made impermeable surfaces generally present, during a relevant heatwave on July 24th, colder values compared to rural areas (Fig. 4). This result is unexpected compared to most studies about UHI spatial variability which are reported in scientific literature. To illustrate this phenomenon, it was found to be useful to ignore the permeable surfaces of the study area as presented in map of Figure 5. By this cartographic output it is possible to visualise only urban areas temperatures characterised by relatively low values symbolised by the blue colour. The estimated temperature values in the entire provincial area range from 27.54 to 50.98 °C. Low values are found mainly in densely vegetated areas, on the coast and in urban centres, while the central area of the province, with lesser influence from maritime winds, experiences higher temperatures, with maximum temperature values corresponding to bare soils.

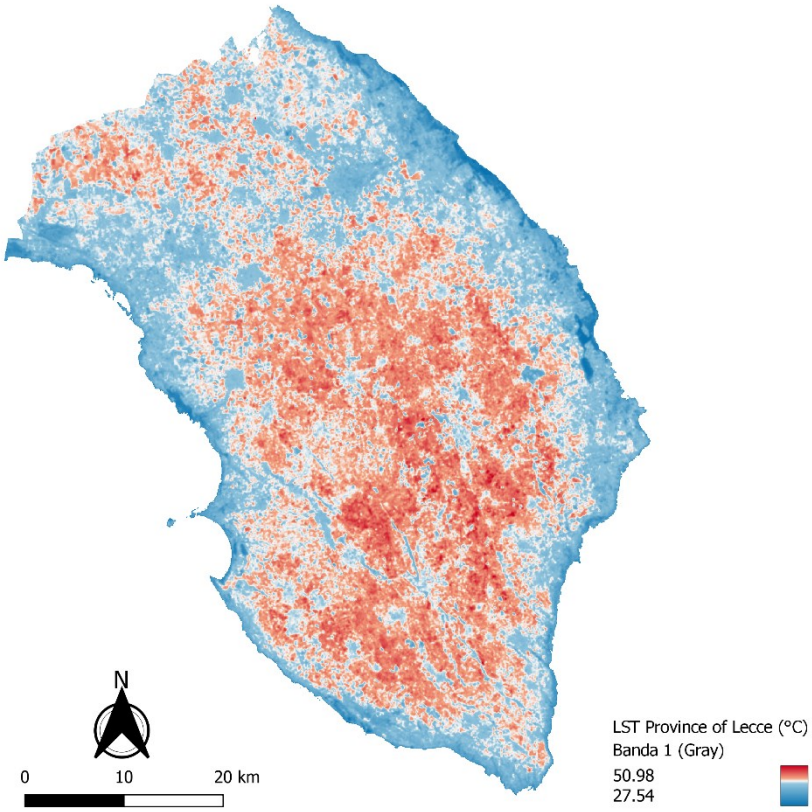

***Figure 4**: Spatial distribution of LST in the Province of Lecce detected on 24th July, 2022.*

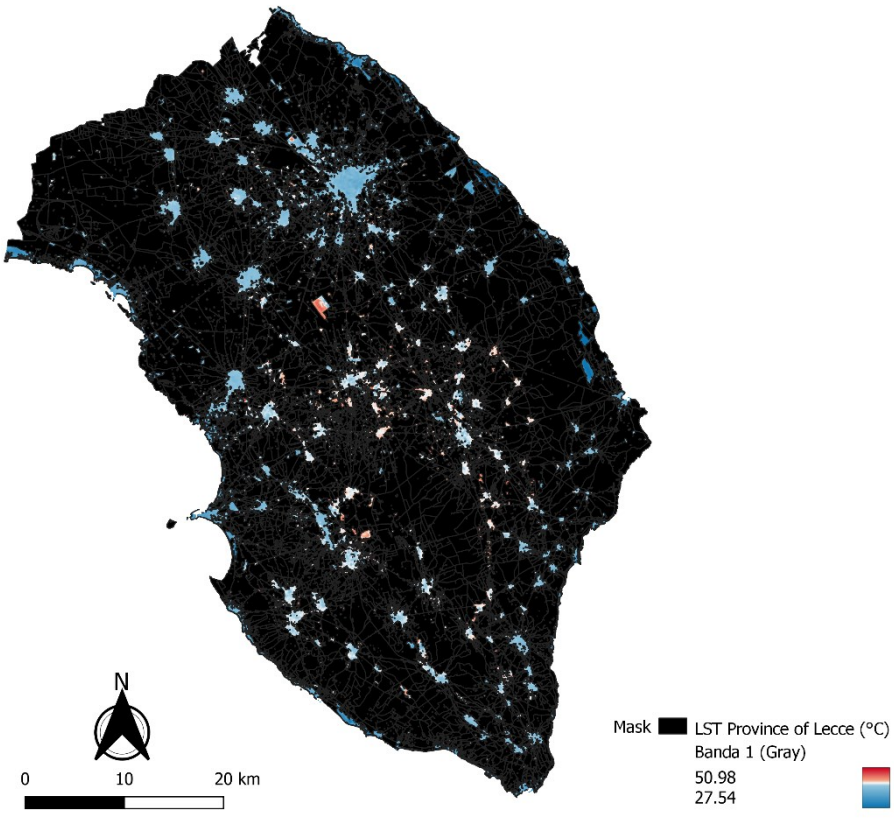

***Figure 5**: LST of impermeable surfaces, mask on permeable surfaces.*

The urban area around Lecce was therefore deeply investigated (Fig. 6) (Fig. 7). It was found that the lowest measured LST is 31.44 °C, while the highest is 48.07 °C. The lowest temperatures are detected in urban areas, especially in the historical centre of the city, in correspondence with urban parks and vegetated areas and along the vegetation in the north-western part of the examined area. Surprisingly, all the industrial areas of the city have low temperatures, with just few exceptions for metal or dark roofs.

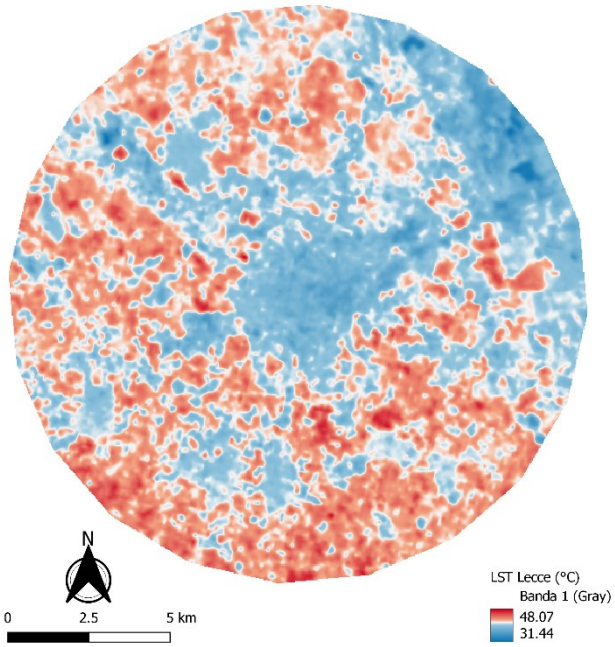

Figure 6: *LST in Lecce detected on 24th July, 2022.*

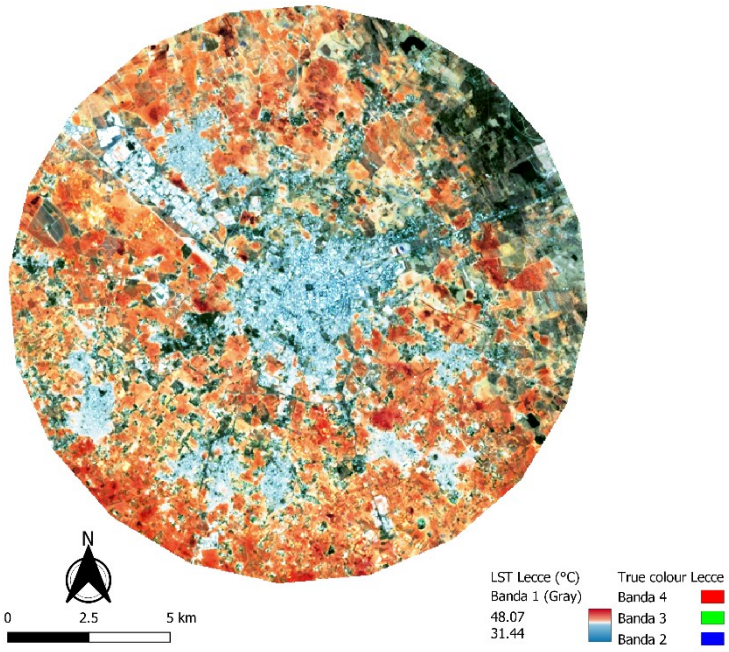

Figure 7*: Spatial distribution of LST in Lecce on 24th July, 2022. It is visible that urban areas are characterised by lower temperatures than rural areas.*

A specific analysis was conducted to understand how vegetation affects surface temperature. In particular, a scatter plot of LST and NDVI values was created for this area (Fig. 8). The results of the linear regression model ($y = a + b * x$) are presented in Table 3 and show that there is a negative linear correlation between LST and NDVI values as the value of R is equal to -0.395.

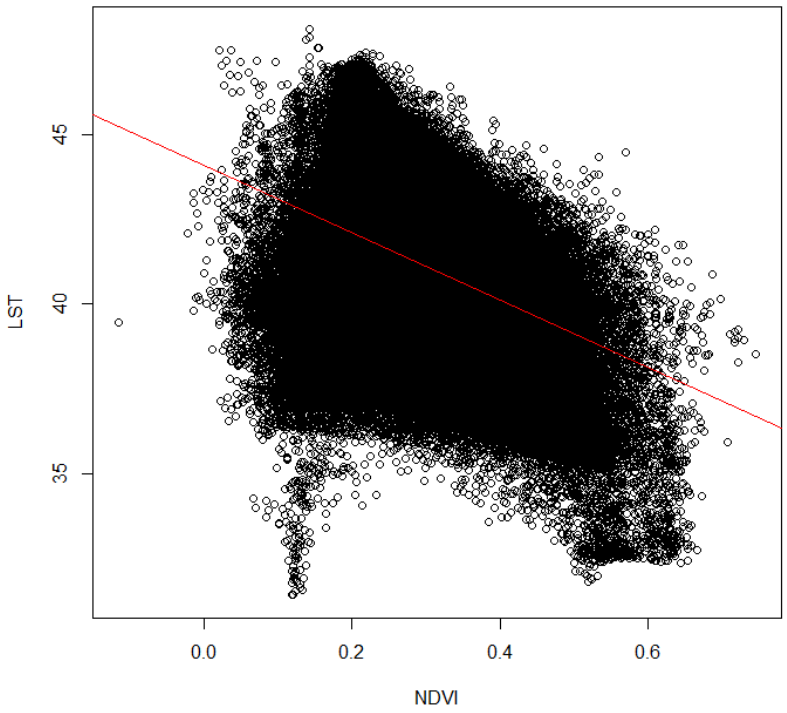

***Figure 8**: Scatter plot of LST-NDVI and linear regression.*

***Table 3**: Linear regression results between LST and NDVI.*

x	y	a	b	R
NDVI	LST	44.08	-9.92	-0.395

It was appropriate to study the behaviour of temperature as a function of the typology of land cover, considering the difference between impermeable and permeable surfaces. The box plot shown in Figure 9 shows that the average temperature measured on impermeable surfaces was 40.32°C, lower than the 41.55°C measured on permeable surfaces. It can clearly be seen that the LST values corresponding to the impermeable surfaces tend to have low values. A Student's t-test confirmed a statistically significant difference between the two means.

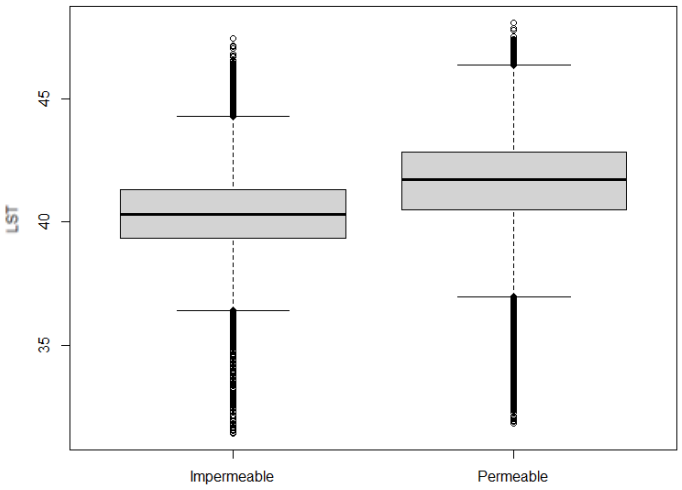

Figure 9: *Box plot of type of surface and temperature (°C). Permeable surfaces include vegetation.*

To go into more detail, it was decided to exclude the pixels belonging to the permeable areas with NDVI values of less than 0.3. This way it was possible to avoid the cooling effect of these areas due to evapotranspiration. Below this threshold, the effects that vegetation has on temperature are negligible. It was found that about 63.3% of the non-urbanised soils have a NDVI value lower than the established threshold. This means that a large part of the ground is bare or sparsely vegetated. The box plot presented in Figure 10 shows that the average surface temperature calculated in these areas is 42.25°C, which is almost 2°C higher than the average temperature calculated for the urbanised areas. Also in this case, the two means show a statistically significant difference.

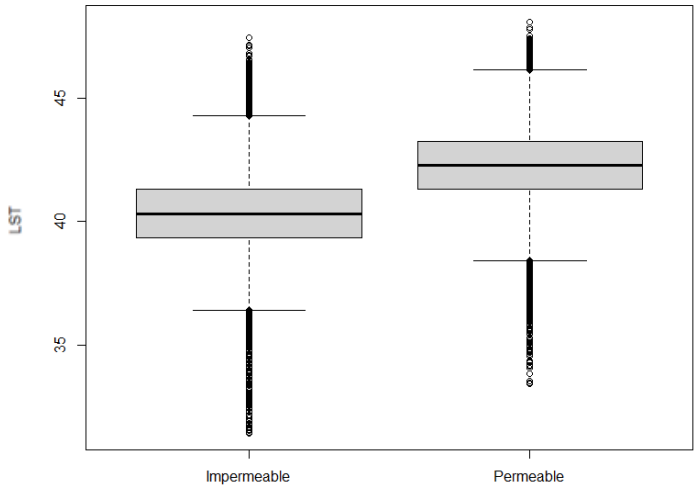

Figure 10*: Box plot of type of surface and temperature (°C). Permeable surfaces do not include vegetation.*

3.4 Urban Heat Island Intensity

In order to obtain a homogeneous distribution of pins within the circular crown around the urban area of Lecce, it was necessary to use a distance threshold of 100 m from urbanised areas, as mentioned in section 2.7. The number of pins came out to be 103 and can be seen in Figure 11. Most of them fall in areas with very high values of LST (Figure 12). The average temperature at these points is 42.48°C, with a minimum of 36.39°C and a maximum of 46.85°C.

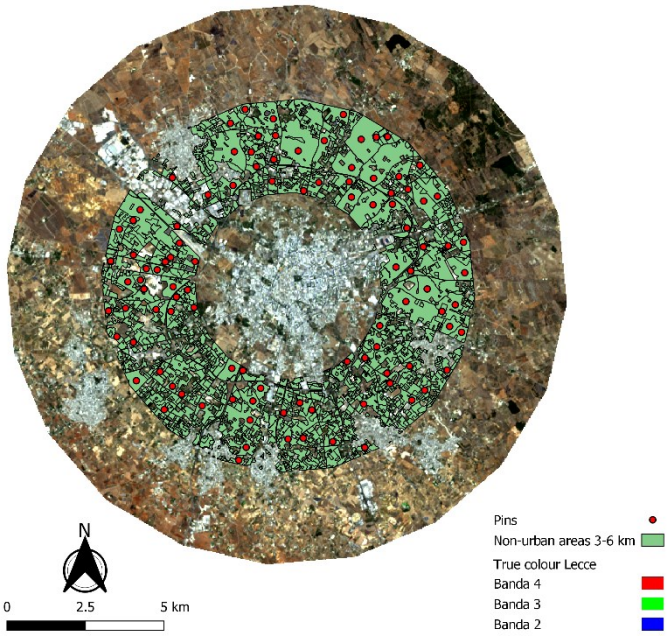

***Figure 11**: Distribution of pins in non-urban areas 3-6 km away from the centre of Lecce.*

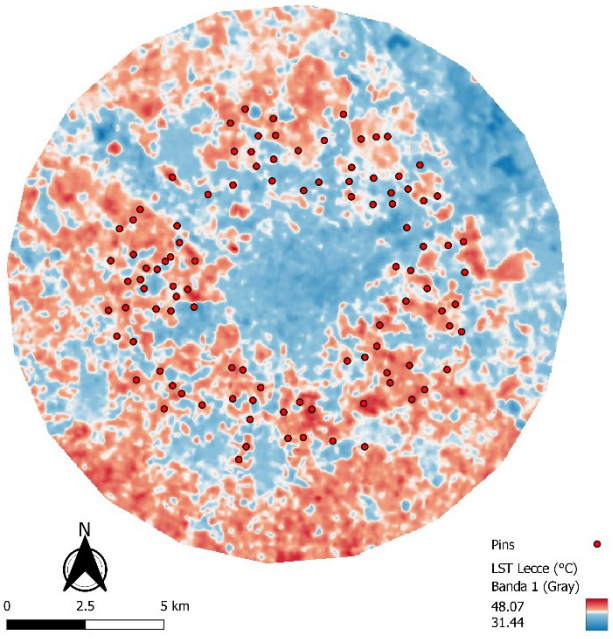

***Figure 12**: Distribution of pins on the LST map. Most of pins are located in warm areas.*

The analysis of pins allows the mapping of the thermal anomaly in the study area with a 100 m raster resolution (Fig. 13) (Fig.14).

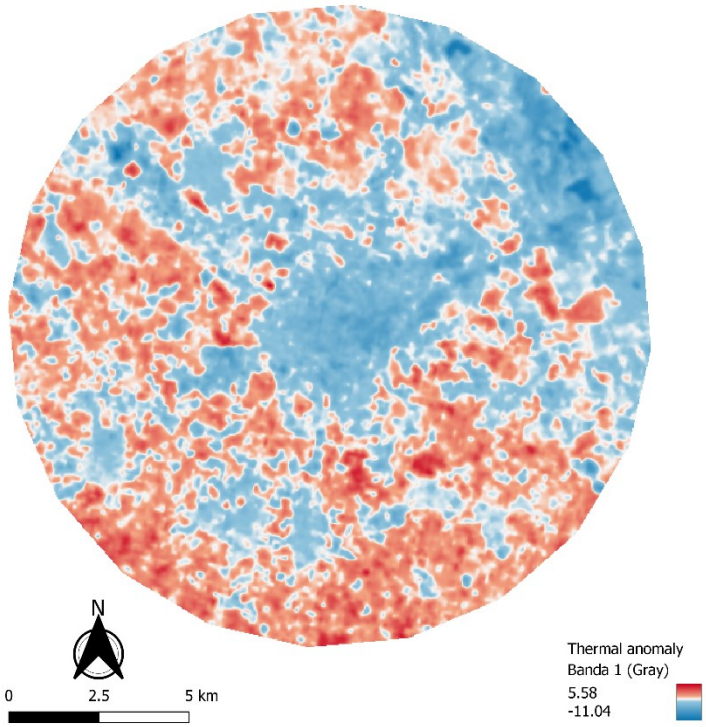

***Figure 13**: Thermal anomaly map in the city of Lecce on 24th July, 2022.*

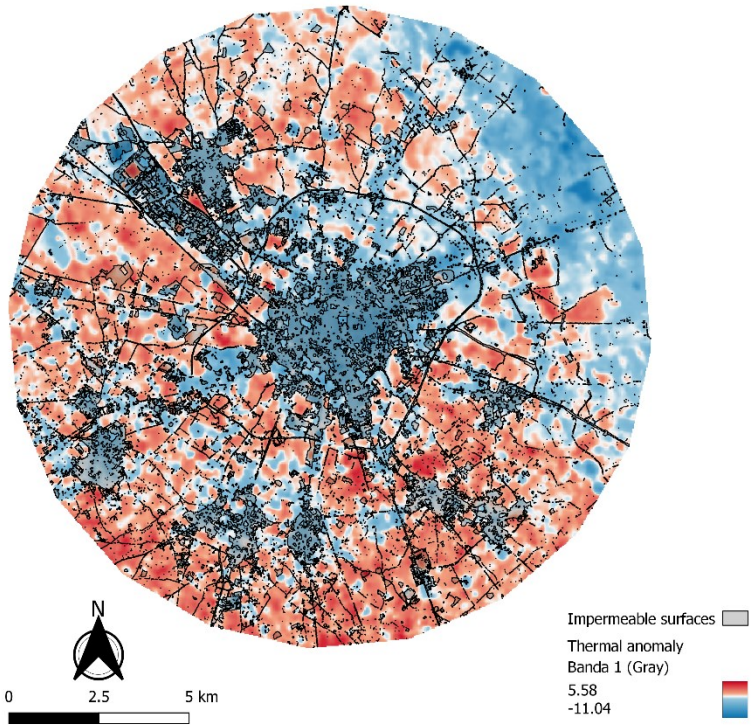

***Figure 14**: Thermal anomaly map in the city of Lecce. Urbanised surfaces have a negative difference of temperature since they are cooler than the average temperature of pins.*

This analysis confirms the previously derived anomalous temperature behaviour. The thermal anomaly in some urbanised areas is truly remarkable, reaching up to 11°C difference. The highest difference value was found in a white limestone quarry. The figure below shows how the temperature seems to be lower in correspondence with bright and highly reflective surfaces such as the quarry, whose rocks constitute the main component of the Salento building material. It is therefore clear that this type of material and the albedo play a role in regulating the surface temperature. In contrast, it is noticeable that the use of metals as roofing material is strongly discouraged because, being excellent conductors of heat, they can easily reach excessively high temperatures. The maximum temperature at the centre of the metal roof displayed in figure 15 was 46.26°C, definitely higher when compared to the 31.44°C measured at the centre of the quarry. The choice of material in the design of urban areas is therefore of great importance; this can be a deciding factor in the success of future sustainable urban areas planning. This research shows how these decisions shaped the environmental effect on urban areas in and around the cities in Salento, where most buildings are not covered with tiles but with limestone rocks, with great benefits in counteracting the phenomenon of urban heat islands.

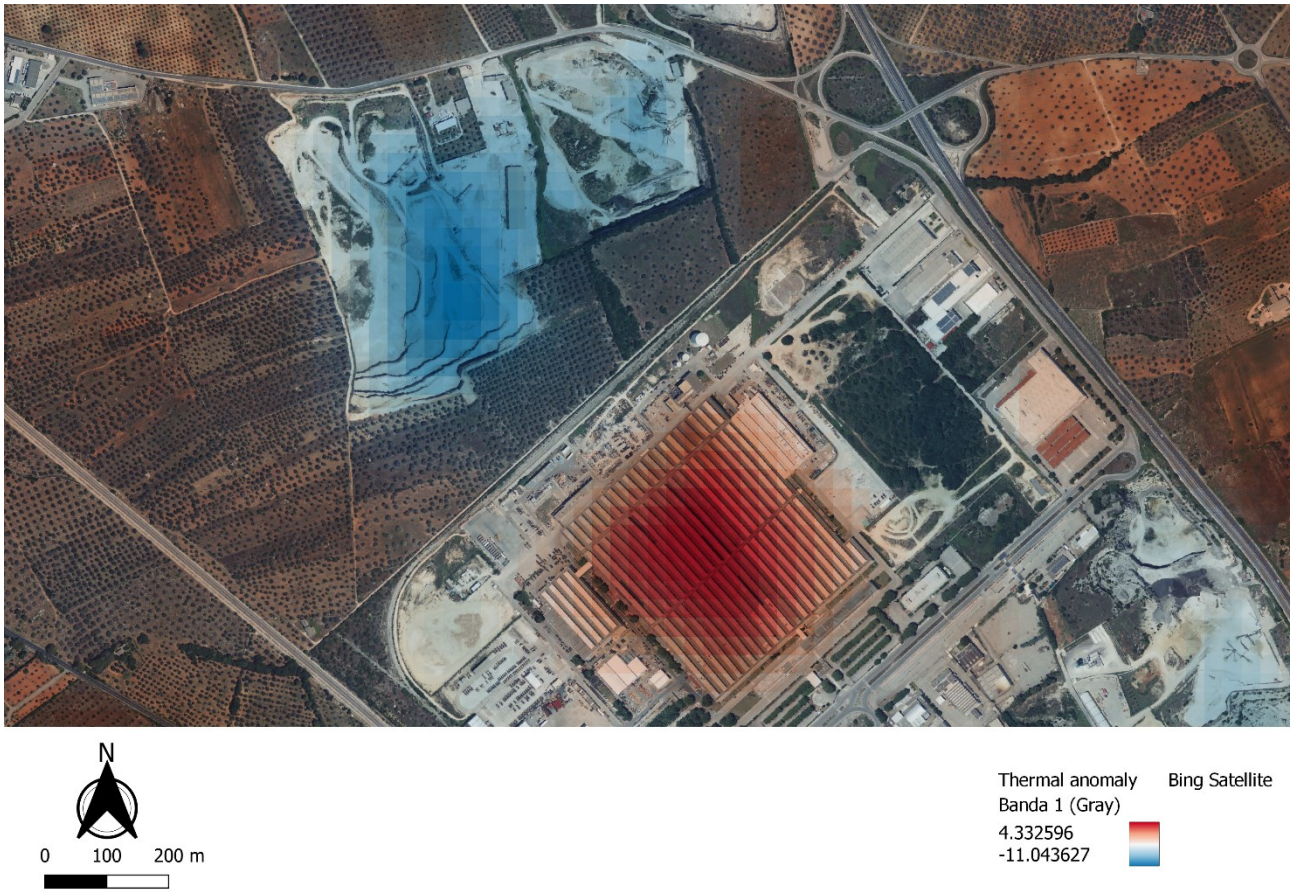

***Figure 15**: Details of thermal anomaly in the industrial area of Lecce.*

3.5 Surface Albedo

The albedo values obtained by applying formula (7) ranged from 0.0924 to 0.922, but only 11 of the calculated pixels had values exceeding the threshold of 0.60. These outliers were identified and subsequently eliminated. The new maximum value adopted by the albedo is 0.582. Figure 16 shows how the albedo in vegetated areas assume very low values. Looking only at impermeable surfaces (Figure 17), it can be seen that buildings have high albedo values, in contrast to asphalt surfaces such as roads or concreted area. These high values are mainly due to the building material, the so-called “pietra leccese”, a locally mined Miocene calcarenite. This factor may be responsible for the thermal anomaly in the towns of Salento.

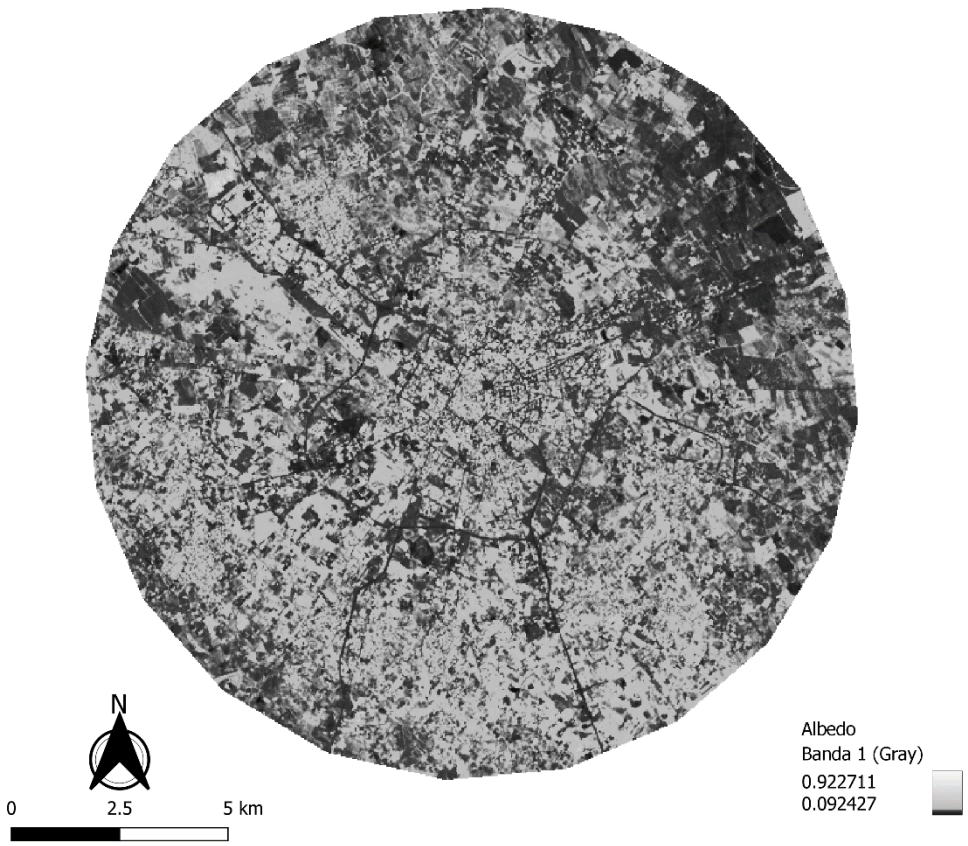

***Figure 16**: Albedo in Lecce.*

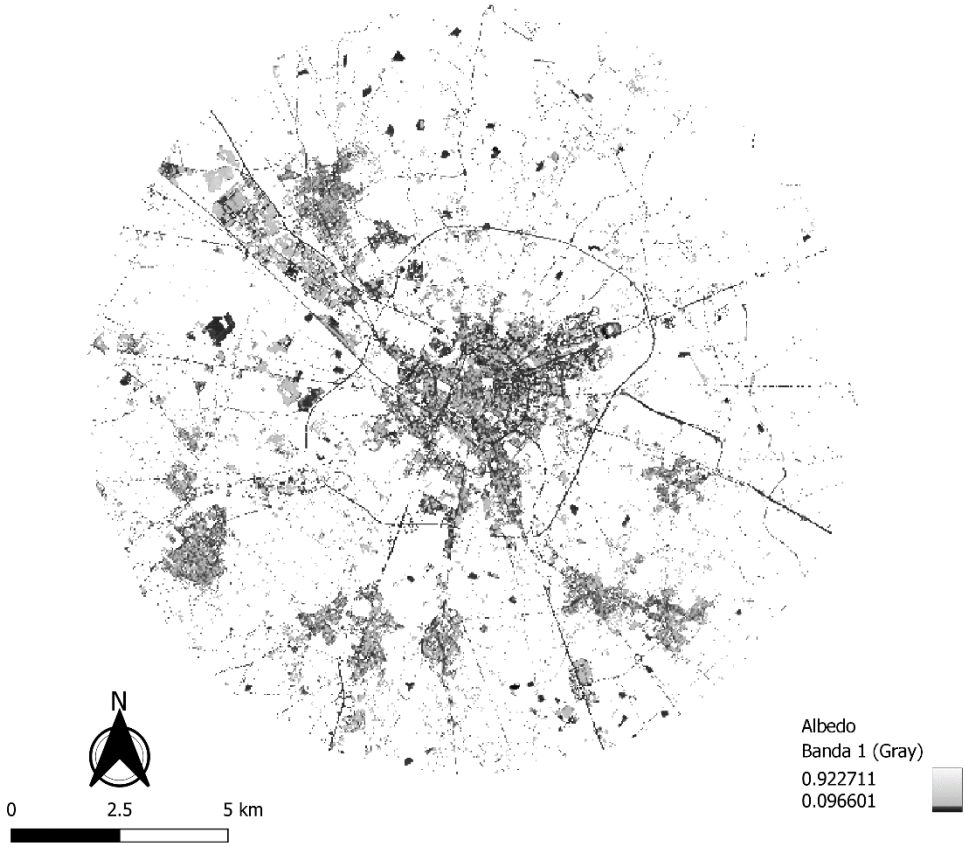

***Figure 17**: Albedo in impermeable areas of Lecce and surroundings.*

It could be determined that the average albedo value of non-vegetated permeable surfaces is 0.205, while the average albedo value of impermeable surfaces is 0.218.

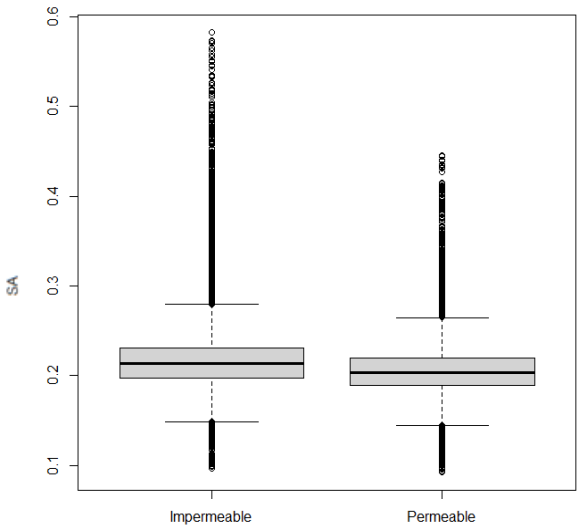

***Figure 18**: Box plot of type of surface and albedo.*

The boxplot in Figure 18 shows that the albedo of permeable surfaces does not exceed values above 0.445, in contrast to the albedo values of impermeable surfaces, which can reach higher values up to

0.582. Although the values assumed by the two means are similar, their difference is statistically significant. The fact that the albedo of non-vegetated areas is about the same as that of urban areas might suggest that albedo does not have much effect on temperature regulation. Actually, the albedo values in Salento urban areas far exceed the average albedo of most cities in the world, and this most likely has an important and clearly visible influence on the surface temperature. However, it must be taken into account that impermeable surfaces also include areas with relatively low albedo values, such as large areas of photovoltaic installations in the Salento landscape, which could influence and lower the average value.

The scatter plot and its associated linear regression in Figure 19 show the expected inverse relationship between LST and the surface albedo. Results are presented in Table 4.

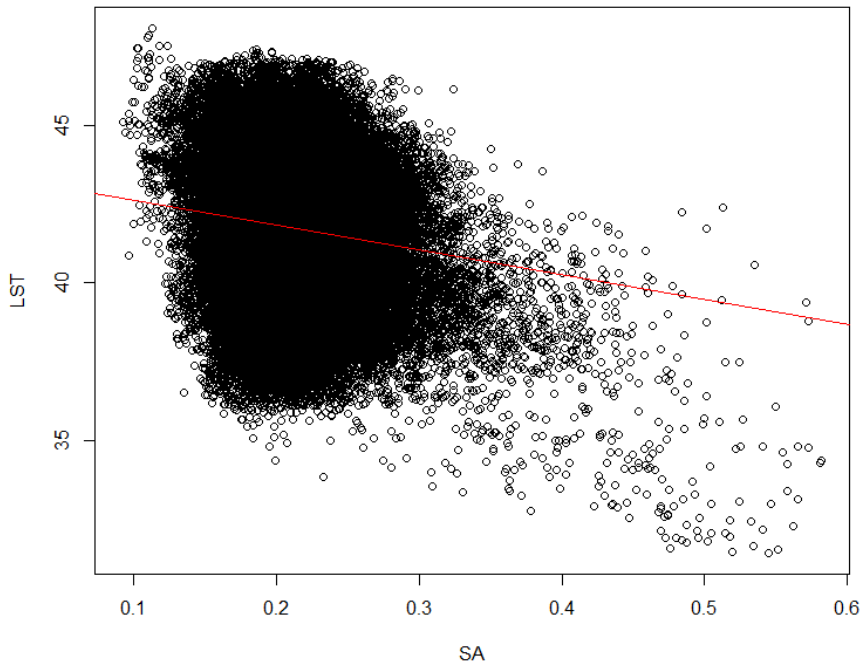

***Figure 19**: Scatter plot of LST-SA and linear regression.*

***Table 4**: Linear regression results between LST and SA.*

x	y	a	b	R
SA	LST	43.42	-7.87	-0.134

Nevertheless, the relationship between the two variables seems weak. A plausible explanation of this can be found in the very similar albedo values of permeable and impermeable surfaces within the study area. In fact, impermeable surfaces reflected on average only 1% more solar radiation than vegetation-free permeable surfaces. A different spatial distribution of temperature would have resulted in significantly lower albedo values of about 0.1 to 0.15, as it is the case in most cities. In this last case, impermeable surfaces would reflect on average 5-10% less solar radiation than permeable surfaces, absorbing more energy and thus heat. Moreover, the temperature difference between built-up areas and the landscape is also due to the sparse, dry or absent vegetation on the ground. All these factors combined lead to what was found and studied in this article.

4. Conclusions

In the present research, UHI and the LST anomalies on July 24th, 2022 were mapped, during one of the two heatwaves that occurred in Salento. It was found that most urban centres and urbanised areas, including industrial areas, respond anomalously to reported UHI spatial analyses, showing lower temperature values than the surrounding rural areas. In the Province of Lecce, the spatial distribution of temperatures is probably influenced by vegetation, proximity to the sea and soil characteristics. Along the coast, where NDVI analysis showed higher values, indicating the presence of more abundant vegetation, temperatures are much lower. The maximum values obtained, with peaks of LST around 50 °C, are mainly located in the central areas of the region and in correspondence with the areas of abandoned and bare agricultural land. Considering Lecce and the surrounding areas within a 9 km radius of the geographic centre of the city as a reference area, it can be seen that about 63.3% of the permeable surfaces have NDVI values below 0.3, which means that more than half of the non-urbanised areas have very little vegetation. This has a probably a relevant impact on LST, as the lack of vegetation in these areas does not allow for cooling by plant evapotranspiration. The average temperature in these areas with sparse vegetation is 42.25 °C, which is a very high value if compared to the average temperature of 40.32 °C experienced on impermeable surfaces. The analysis of thermal anomalies in the Lecce area confirmed this temperature anomaly, highlighting that temperatures in urban areas can be up to 11 °C lower than in surrounding rural areas. The lowest temperature value of 31.44 °C was found near a quarry of white limestone, highlighting the role of material type and albedo in controlling temperature. Analysing the surface albedo, high values were found in the urban areas of Lecce, with values certainly above the average of world cities. A relationship between surface albedo and temperature was found. Its

role was, however, marginal, probably because of the similarity in the values of albedo in impermeable areas and on non-vegetated permeable surfaces; thus it can be concluded that albedo plays a significant role in the regulation of surface temperature in Salento cities. Of great importance for this study was the almost total absence of vegetation in the countryside of Salento during the summer months, exposing the soil to more solar radiation and heat. It would be advisable to find strategic solutions to keep temperatures in these areas lower than they currently are, for example by increasing the areas used for agriculture or, in some cases, to cultivate these areas with simple grass.

Bibliography

Akbari, H., Damon Matthews, H., & Seto, D. (2012). The long-term effect of increasing the albedo of urban areas. *Environmental Research Letters*, *7*(2). https://doi.org/10.1088/1748-9326/7/2/024004

Armson, D., Stringer, P., & Ennos, A. R. (2012). The effect of tree shade and grass on surface and globe temperatures in an urban area. *Urban Forestry and Urban Greening*, *11*(3), 245–255. https://doi.org/10.1016/J.UFUG.2012.05.002

Beniston, M., Stephenson, D. B., Christensen, O. B., Ferro, C. A. T., Frei, C., Goyette, S., Halsnaes, K., Holt, T., Jylhä, K., Koffi, B., Palutikof, J., Schöll, R., Semmler, T., Woth, K., Beniston, M., Goyette, S., Stephenson, D. B., Ferro, C. A. T., Christensen, O. B., … Woth, K. (2007). Future extreme events in European climate: an exploration of regional climate model projections. *Climatic Change*, *81*, 71–95. https://doi.org/10.1007/s10584-006-9226-z

Bonafoni, S., Baldinelli, G., Rotili, A., & Verducci, P. (2017, May 10). Albedo and surface temperature relation in urban areas: Analysis with different sensors. *2017 Joint Urban Remote Sensing Event, JURSE 2017*. https://doi.org/10.1109/JURSE.2017.7924612

Bounoua, L., Zhang, P., Mostovoy, G., Thome, K., Masek, J., Imhoff, M., Shepherd, M., Quattrochi, D., Santanello, J., Silva, J., Wolfe, R., & Toure, A. M. (2015). Impact of urbanization on US surface climate. *Environmental Research Letters*, *10*(8). https://doi.org/10.1088/1748-9326/10/8/084010

Cunha, J., Nóbrega, R. L. B., Rufino, I., Erasmi, S., Galvão, C., & Valente, F. (2020). Surface albedo as a proxy for land-cover clearing in seasonally dry forests: Evidence from the Brazilian Caatinga. *Remote Sensing of Environment*, *238*. https://doi.org/10.1016/j.rse.2019.111250

Diffenbaugh, N. S., Pal, J. S., Giorgi, F., & Gao, X. (2007). Heat stress intensification in the Mediterranean climate change hotspot. *Geophysical Research Letters*, *34*(11). https://doi.org/10.1029/2007GL030000

D'ippoliti, D., Michelozzi, P., Marino, C., De'donato, F., Menne, B., Katsouyanni, K., Kirchmayer, U., Analitis, A., Medina-Ramón, M., Paldy, A., Atkinson, R., Kovats, S., Bisanti, L., Schneider, A., Lefranc, A., Iñiguez, C., & Perucci, C. A. (2010). *The impact of heat waves on*

mortality in 9 European cities: results from the EuroHEAT project. http://www.ehjournal.net/content/9/1/37

Ghosh, S., & Das, A. (2018). Modelling urban cooling island impact of green space and water bodies on surface urban heat island in a continuously developing urban area. *Modeling Earth Systems and Environment*, *4*(2), 501–515. https://doi.org/10.1007/s40808-018-0456-7

Guerreiro, S. B., Dawson, R. J., Kilsby, C., Lewis, E., & Ford, A. (2018). Future heat-waves, droughts and floods in 571 European cities. *Environmental Research Letters*, *13*(3), 034009. https://doi.org/10.1088/1748-9326/AAAAD3

Kim, S. W., & Brown, R. D. (2021). Urban heat island (UHI) variations within a city boundary: A systematic literature review. *Renewable and Sustainable Energy Reviews*, *148*, 111256. https://doi.org/10.1016/J.RSER.2021.111256

Kshetri, T. B. (2018). *Land Use/Land Cover Map of Pokhara: 2018 View project Volume II Geomatics for Sustainable Development NDVI, NDBI AND NDWI CALCULATION USING LANDSAT 7 AND 8*. https://www.researchgate.net/publication/327971920

Kumar, D., & Shekhar, S. (2015). Statistical analysis of land surface temperature-vegetation indexes relationship through thermal remote sensing. *Ecotoxicology and Environmental Safety*, *121*, 39–44. https://doi.org/10.1016/J.ECOENV.2015.07.004

Lionello, P., & Scarascia, L. (2018). The relation between climate change in the Mediterranean region and global warming. *Regional Environmental Change*, *18*(5), 1481–1493. https://doi.org/10.1007/s10113-018-1290-1

Liu, L., & Zhang, Y. (2005). Remote Sensing Urban Heat Island Analysis Using the Landsat TM Data and ASTER Data: A Case Study in Hong Kong. *Remote Sens*, *3*, 1535–1552. https://doi.org/10.3390/rs3071535

Mohajerani, A., Bakaric, J., & Jeffrey-Bailey, T. (2017). The urban heat island effect, its causes, and mitigation, with reference to the thermal properties of asphalt concrete. *Journal of Environmental Management*, *197*, 522–538. https://doi.org/10.1016/J.JENVMAN.2017.03.095

Narayana Reddy, S., & Manikiam, B. (2017). Land Surface Temperature Retrieval from LANDSAT data using Emissivity Estimation. In *International Journal of Applied Engineering Research* (Vol. 12). http://www.ripublication.com

Naumann, G., & Formetta, G. (2020). *Global warming and human impacts of heat and cold extremes in the EU Resilience of large investments and critical infrastructures in Europe to climate change (CCMFF) View project Nodo AV Firenze View project*. https://doi.org/10.2760/47878

Ni, J., Cheng, Y., Wang, Q., Ng, C. W. W., & Garg, A. (2019). Effects of vegetation on soil temperature and water content: Field monitoring and numerical modelling. *Journal of Hydrology*, *571*, 494–502. https://doi.org/10.1016/J.JHYDROL.2019.02.009

Oke, T. R. (1982). The energetic basis of the urban heat island. In *Quart. J. R. Met. Soc* (Vol. 108, Issue 455).

Oudin Åström, D., Schifano, P., Asta, F., Lallo, A., Michelozzi, P., Rocklöv, J., & Forsberg, B. (2015). The effect of heat waves on mortality in susceptible groups: A cohort study of a mediterranean and a northern European City. *Environmental Health: A Global Access Science Source*, *14*(1). https://doi.org/10.1186/s12940-015-0012-0

Rajeshwari, A., & Mani N, D. (2014). ESTIMATION OF LAND SURFACE TEMPERATURE OF DINDIGUL DISTRICT USING LANDSAT 8 DATA. *IJRET: International Journal of Research in Engineering and Technology*, 2321–7308. http://www.ijret.org

Russo, S., Dosio, A., Graversen, R. G., Sillmann, J., Carrao, H., Dunbar, M. B., Singleton, A., Montagna, P., Barbola, P., & Vogt, J. v. (2014). Magnitude of extreme heat waves in present climate and their projection in a warming world. *Journal of Geophysical Research Atmospheres*, *119*(22), 12,500-12,512. https://doi.org/10.1002/2014JD022098

Sangiorgio, V., Fiorito, F., & Santamouris, M. (2020). Development of a holistic urban heat island evaluation methodology. *Scientific Reports*, *10*(1). https://doi.org/10.1038/s41598-020-75018-4

Schlesinger, W. H., Dietze, M. C., Jackson, R. B., Phillips, R. P., Rhoades, C. C., Rustad, L. E., & Vose, J. M. (2016). Forest biogeochemistry in response to drought. *Global Change Biology*, *22*(7), 2318–2328. https://doi.org/10.1111/GCB.13105

Souch, C. A., & Souch, C. (1993). THE EFFECT OF TREES ON SUMMERTIME BELOW CANOPY URBAN CLIMATES: A CASE STUDY BLOOMINGTON, INDIANA. In *Journal of Arboriculture* (Vol. 19, Issue 5).

Spano, D. (2020). *Analisi del rischio I cambiamenti climatici in Italia*.

Stathopoulou, M., & Cartalis, C. (2007). Daytime urban heat islands from Landsat ETM+ and Corine land cover data: An application to major cities in Greece. *Solar Energy*, *81*(3), 358–368. https://doi.org/10.1016/J.SOLENER.2006.06.014

Taha, H. (1997). Urban climates and heat islands: albedo, evapotranspiration, and anthropogenic heat. In *Energy and Buildings* (Vol. 25).

Tan, J., Zheng, Y., Tang, X., Guo, C., Li, L., Song, G., Zhen, X., Yuan, D., Kalkstein, A. J., Li, F., & Chen, & H. (n.d.). *The urban heat island and its impact on heat waves and human health in Shanghai*. https://doi.org/10.1007/s00484-009-0256-x

Todeschi, V., Javanroodi, K., Castello, R., Mohajeri, N., Mutani, G., & Scartezzini, J. L. (2022). Impact of the COVID-19 pandemic on the energy performance of residential neighborhoods and their occupancy behavior. *Sustainable Cities and Society*, *82*. https://doi.org/10.1016/J.SCS.2022.103896

USGS. (n.d.). Https://Www.Usgs.Gov/Landsat-Missions/Landsat-8.

Wehrli, K., Guillod, B. P., Hauser, M., Leclair, M., & Seneviratne, S. I. (2019). Identifying Key Driving Processes of Major Recent Heat Waves. *Journal of Geophysical Research: Atmospheres*, *124*(22), 11746–11765. https://doi.org/10.1029/2019JD030635

Yang, X., Lu, M., Wang, Y., Wang, Y., Liu, Z., Chen, S., Toscano, S., Franzoni, G., & Álvarez, S. (2021). *horticulturae Response Mechanism of Plants to Drought Stress*. https://doi.org/10.3390/horticulturae7030050

Sitography

https://www.isprambiente.gov.it/it/attivita/suolo-e-territorio/suolo/copertura-del-suolo

https://www.usgs.gov/landsat-missions/landsat-8

https://earthexplorer.usgs.gov

https://dati.puglia.it/ckan/dataset/uso-del-suolo-2011-uds

https://www.usgs.gov/landsat-missions/using-usgs-landsat-level-1-data-product

https://www.ncei.noaa.gov/access/search/data-search/global-summary-of-the-day?stations=16332099999&dataTypes=MAX&dataTypes=MIN&dataTypes=TEMP